

Dynamical and magnetic field time constants for Titan's ionosphere: Empirical estimates and comparisons with Venus

T. E. Cravens,¹ M. Richard,¹ Y.-J. Ma,² C. Bertucci,³ J. G. Luhmann,⁴ S. Ledvina,⁴ I. P. Robertson,¹ J.-E. Wahlund,⁵ K. Ågren,⁵ J. Cui,⁶ I. Muller-Wodarg,⁶ J. H. Waite,⁷ M. Dougherty,⁶ J. Bell,⁷ and D. Ulusen⁴

Received 2 November 2009; revised 7 April 2010; accepted 15 April 2010; published 27 August 2010.

[1] Plasma in Titan's ionosphere flows in response to forcing from thermal pressure gradients, magnetic forces, gravity, and ion-neutral collisions. This paper takes an empirical approach to the ionospheric dynamics by using data from Cassini instruments to estimate pressures, flow speeds, and time constants on the dayside and nightside. The plasma flow speed relative to the neutral gas speed is approximately 1 m s^{-1} near an altitude of 1000 km and 200 m s^{-1} at 1500 km. For comparison, the thermospheric neutral wind speed is about 100 m s^{-1} . The ionospheric plasma is strongly coupled to the neutrals below an altitude of about 1300 km. Transport, vertical or horizontal, becomes more important than chemistry in controlling ionospheric densities above about 1200–1500 km, depending on the ion species. Empirical estimates are used to demonstrate that the structure of the ionospheric magnetic field is determined by plasma transport (including neutral wind effects) for altitudes above about 1000 km and by magnetic diffusion at lower altitudes. The paper suggests that a velocity shear layer near 1300 km could exist at some locations and could affect the structure of the magnetic field. Both Hall and polarization electric field terms in the magnetic induction equation are shown to be locally important in controlling the structure of Titan's ionospheric magnetic field. Comparisons are made between the ionospheric dynamics at Titan and at Venus.

Citation: Cravens, T. E., et al. (2010), Dynamical and magnetic field time constants for Titan's ionosphere: Empirical estimates and comparisons with Venus, *J. Geophys. Res.*, 115, A08319, doi:10.1029/2009JA015050.

1. Introduction

[2] The coupled ionosphere-magnetosphere dynamics at Titan are difficult to understand for several reasons. The geometry is complicated because the direction to the Sun and the direction of Saturn's magnetospheric flow relative to Titan can differ greatly from one Cassini flyby to another. The spherical nature of Titan's neutral atmosphere also makes analysis more difficult since it is not easy to separate vertical (i.e., radial) and horizontal variations of ionospheric variables along the Cassini spacecraft track. Several approaches to understanding Titan's ionosphere are needed, including 3-D global models of both the neutrals and the

plasma [e.g., Ledvina and Cravens, 1998; Ma et al., 2004, 2006, 2007; Ma, 2008; Brecht et al., 2000; Modolo and Chanteur, 2008; Kabin et al., 1999; Ledvina et al., 2008], but in this paper we take a simple empirical approach to the dynamics and magnetic field by using data from several Cassini instruments. We estimate thermal and magnetic pressures, and using these pressures we estimate flow speeds and time constants in the ionosphere for some dayside (T17 and T18) and nightside (T5) Cassini flybys.

[3] Plasma in Titan's ionosphere flows in response to forcing associated with thermal pressure gradients, magnetic forces (i.e., $\mathbf{J} \times \mathbf{B}$, where \mathbf{J} is the current density and \mathbf{B} is the magnetic field), gravity, and ion-neutral collisions. The flow of ions and electrons plays a key role in controlling densities, the magnetic field, and temperatures in the ionosphere. The magnetic field is induced in the ionosphere as part of the interaction of the ionosphere with the external plasma flow in Saturn's magnetosphere. Ionizing solar radiation affects the dynamics by creating ionospheric plasma on the dayside, thus resulting in day-to-night pressure gradient forces.

[4] *Ip* [1990] used a 1-D single-fluid MHD approach and Keller et al. [1994] used a 1-D multifluid (five ion species, each with their own velocity and density) MHD approach to predict that on the ramside magnetic flux was carried by

¹Department of Physics and Astronomy, University of Kansas, Lawrence, Kansas, USA.

²Institute of Geophysics and Planetary Physics, University of California, Los Angeles, California, USA.

³Instituto de Astronomía y Física del Espacio, Buenos Aires, Argentina.

⁴Space Sciences Laboratory, University of California, Berkeley, California, USA.

⁵Swedish Institute of Space Physics, Uppsala, Sweden.

⁶Space and Atmospheric Physics Group, Blackett Laboratory, Imperial College London, London, UK.

⁷Southwest Research Institute, San Antonio, Texas, USA.

Table 1. Geometrical Information for Cassini Flybys Used in This Study

Flyby Flow	Solar Zenith Angle	External	Latitude	Magnet. Cond. ^a (Saturn Local Time)
T5out	130° (night)	ram	polar	Plasmasheet (5.27)
T17in	30° (day)	wake	low lat.	Unclassif./bimod (2.27)
T18out	85° (day/terminator)	flank	high lat.	Lobe-like (2.27)

^aMagnetospheric conditions from *Rymer et al.* [2009].

downward plasma motion from the magnetic barrier into the ionosphere. This scenario is similar to what happens at Venus during high solar wind dynamic pressure conditions (see review by *Luhmann and Cravens* [1991], *Cravens et al.* [1984], *Shinagawa et al.* [1987], and *Shinagawa and Cravens* [1988]). *Keller and Cravens* [1994] applied a five species hydrodynamic code to the wakeside ionosphere (assuming radial magnetic field lines) and found that the plasma flow was mainly upward and became supersonic in the topside ionosphere. These geometrically simple 1-D MHD models were followed by a multispecies 2-D MHD model [*Cravens et al.*, 1998] and a single-fluid, 3-D MHD model [*Ledvina and Cravens*, 1998]. *Ledvina and Cravens* [1998] showed that Saturn's magnetic field drapes around Titan, forming a magnetotail including Alfvén wings, in qualitative agreement with the picture of the Titan interaction derived from the Voyager 1 encounter data [cf. *Neubauer et al.*, 1984]. The *Ledvina and Cravens* 3-D MHD code had low spatial resolution and did not include a realistic ionosphere, but this model was soon followed by higher-resolution MHD simulations [*Kabin et al.*, 1999; *Ma et al.*, 2004, 2006, 2007]. *Ma* and coworkers's 3-D MHD simulations [*Ma et al.*, 2004, 2006, 2007] are single-fluid (i.e., momentum equation) and multispecies (seven ion-species continuity equations) and take into account ionospheric processes by including ion-neutral collisions, ion production, and ion loss (i.e., chemistry). More recently, *Ma et al.* [2007] included Hall terms, which appear to be important for the Titan interaction. *Backes et al.* [2005] and *Neubauer et al.* [2006] also described models of Titan's interaction and the associated magnetic field structure. Hybrid simulations have also been carried out for the Titan interaction in order to account for the large gyroradii of heavy ions in the upstream magnetospheric flow [e.g., *Brecht et al.*, 2000; *Sillanpaa et al.*, 2006; *Simon et al.*, 2007; *Modolo and Chanteur*, 2008], but these simulations have rather low resolution and do not deal with ionospheric processes very well.

[5] Plasma and field measurements have been made by instruments onboard Cassini [cf. *Hartle et al.*, 2006] for many Titan flybys. The overall view first formed with Voyager 1 measurements (and subsequent modeling and interpretation) was that the incident plasma flow was submagnetosonic and was diverted around the obstacle formed by Titan without a bow shock but with draped magnetic field and a magnetotail. The Cassini mission has confirmed the Voyager picture that there are induced magnetic fields near Titan, but Cassini also made the first measurements of magnetic field in the ionosphere itself. Many details of the external plasma interaction with Titan still elude explanation, and in particular, the structure of the ionospheric magnetic field (and the associated dynamics). And Cassini

measurements demonstrate that the upstream magnetospheric conditions at Titan vary significantly from flyby to flyby (see the review chapters by *Gombosi et al.* [2009] and by *Mitchell et al.* [2009]).

[6] Even when 3-D plasma simulations (see earlier references) generate results that agree with measurements made by the Cassini Orbiter along the spacecraft trajectory, a simple physical interpretation of these results (at least for the ionosphere) has been difficult to formulate. Part of the problem is the complicated mix of solar and external flow geometries alluded to earlier. For example, for the T5 Cassini flyby of Titan, the subsolar point and the subram (for the external flow) point were on the opposite sides of the satellite, whereas for the T18 flyby the subsolar point was about 90° from the subram point. For different flybys the upstream magnetospheric conditions are also different [e.g., *Hartle et al.*, 2006], depending on where Titan is in its orbit and whether or not it is in the plasmasheet or lobes of Saturn [*Rymer et al.*, 2009; *Bertucci et al.*, 2008, 2009]. Another part of the problem might be that, for the ionospheric part of the plasma interaction, a great variety of physical processes are contributing to the dynamics and to the structure of the magnetic field. Not all these processes are included in every numerical model. For example, some numerical models of the plasma interaction do not allow magnetic diffusion through the lower boundary and, thus, into the lower atmosphere.

[7] The hope for the current paper is that the empirical estimates being described will help in the interpretation of Cassini data and numerical simulations pertaining to the ionospheric part of the Titan plasma environment. Section 2 of the paper contains a brief review of some relevant magnetohydrodynamic (MHD) theory. Section 3 presents some Cassini plasma and field data for T5, T17, and T18. Section 4 presents our empirical estimates of ionospheric plasma flow speeds and the associated time constants, calculated using the Cassini data. Sections 5 and 6 discuss the implications of these estimates for Titan's ionospheric plasma and magnetic field structure, respectively. Section 7 is a brief summary of the results.

2. MHD Theory for Titan's Ionosphere

[8] The ionosphere of Titan contains a large number of ion species as well as electrons [cf. *Cravens et al.*, 2006; *Wahlund et al.*, 2005; *Coates et al.*, 2007]. In a fully multifluid plasma description, all species have their own densities, velocities, and temperatures [cf. *Schunk and Nagy*, 2000; *Cravens*, 1997]. In the current paper, we use a single-fluid MHD approach [cf. *Cravens et al.*, 1997] to estimate the overall flow velocity of the ionospheric plasma and the associated time constants.

2.1. Single-Fluid Momentum Equation

[9] The single-fluid momentum equation can be written as [cf. *Cravens*, 1997]:

$$\rho \left(\frac{\partial \mathbf{u}}{\partial t} + \mathbf{u} \cdot \nabla \mathbf{u} \right) = -\nabla(p_e + p_i) + \mathbf{J} \times \mathbf{B} + \rho \mathbf{g} + \rho \nu_{in} (\mathbf{u} - \mathbf{u}_n) \quad (1)$$

where \mathbf{u} is the single-fluid plasma flow velocity, ρ is the mass density of the plasma (i.e., the sum of $m_s n_s$ over all ion species s), \mathbf{B} is the magnetic field, \mathbf{J} is the current density, ν_{in} is the ion-neutral momentum transfer collision frequency, and \mathbf{u}_n is the neutral flow velocity. The single-fluid flow velocity is well-approximated by the sum of $m_s n_s \mathbf{u}_s$ over all ion species, divided by the total mass density of the plasma. The value of m_s is the mass of ion species s and \mathbf{u}_s is the velocity of this species. The thermal pressures for electrons and ions are given by $p_e = n_e k_B T_e$ and $p_i = n_i k_B T_i$, respectively. The total ion density is denoted n_i and by quasi-neutrality is assumed to be equal to the electron density, n_e (in the absence of negative ion species). The value of k_B is Boltzmann's constant, and T_e and T_i are the electron and ion temperatures, respectively. Equation (1) describes the acceleration of a parcel of plasma in response to the net force per unit volume on this parcel. The magnetic field in a MHD description is found using the magnetic induction equation (Faraday's law plus a generalized Ohm's law).

[10] The Lorentz force term in equation (1) is often rewritten using Ampere's law (minus the displacement current):

$$\mathbf{J} \times \mathbf{B} = -\nabla \left(\frac{B^2}{2\mu_0} \right) + \frac{1}{\mu_0} \mathbf{B} \cdot \nabla \mathbf{B}. \quad (2)$$

The quantity $B^2/2\mu_0$ is "magnetic pressure", p_B , which can be grouped with the thermal pressure in equation (1) to give a total pressure.

[11] For slow (i.e., submagnetosonic) ionospheric flow, the following simple expression for the velocity can be found using equation (1):

$$\mathbf{u} - \mathbf{u}_n = \frac{1}{\rho \nu_{in}} [-\nabla(p_e + p_i) + \mathbf{J} \times \mathbf{B} + \rho \mathbf{g}]. \quad (3)$$

The ion-neutral momentum transfer collision frequency ($\nu_{in} = k_{in} n_n$) is proportional to the neutral density and decreases rapidly as altitude increases. We use collision coefficients (k_{in}) for N_2 and CH_4 from *Keller et al.* [1994] [also see *Schunk and Nagy*, 2000]. Note that if $\rho \nu_{in}$ is large enough (i.e., which happens in Titan's ionosphere below about 1300 km), then the term in brackets is small and the plasma is tied to the neutral gas (i.e., $\mathbf{u} \approx \mathbf{u}_n$).

[12] In this paper, we use equation (3) to roughly estimate the quantity $\mathbf{u}' = |\mathbf{u} - \mathbf{u}_n|$ using empirical data in several ways. Cassini measurements are obtained along the spacecraft path and do not by themselves provide a 3-D, or time-dependent, picture of these quantities. For example, the direction of the pressure gradient force is not entirely obvious from the measured variation of pressure along the spacecraft path. Either physical reasoning or global modeling can be applied to remedy this deficiency. For some of our estimates (e.g., for T17) based on equation (3), we assume that the gradients are primarily vertical (i.e., radial) and we roughly determine numerically the derivative of pressure with respect to altitude. A vertically directed pressure gradient is probably a reasonable assumption in the middle of the dayside (i.e., T17) where photoionization by solar radiation dominates the overall ion production. For other estimates we simply approximate the pressure gradient as "measured" pressure divided by a "reasonable" scale-

length (L). As will be discussed later, we will use two different estimates of L —one for typical vertical scales ($L \approx L_{\text{ver}}$) and another for typical horizontal scales ($L \approx L_{\text{hor}}$). A rough estimate of \mathbf{u}' is thus obtained (neglecting the gravity term in equation (3)) and is given by:

$$|\mathbf{u}'| = |\mathbf{u} - \mathbf{u}_n| \approx \frac{p_{\text{thermal}} + p_B}{L \rho \nu_{in}} \quad (4)$$

The $\mathbf{J} \times \mathbf{B}$ term for this expression was approximated as magnetic pressure ($p_B = B^2/2\mu_0$) divided by a length-scale L , and the thermal pressure gradient force was approximated as thermal pressure ($p_{\text{thermal}} = p_e + p_i$) divided by a length-scale L . We separately estimated the vertical flow speed produced by the gravity term alone (i.e., this would apply if the total pressure was uniform): $\mathbf{u}' \approx g/\nu_{in}$ (downward). "Transport" time constants can be obtained from the flow speed estimates using $\tau \approx L/u$ where L is again either L_{ver} or L_{hor} .

2.2. Magnetic Induction Equation

[13] Magnetic fields were observed in Titan's ionosphere and are induced by the interaction of the external magnetized plasma flow with the ionosphere. In MHD theory Faraday's law is used to determine the evolution of the magnetic field [cf. *Siscoe*, 1983; *Cravens*, 1997]:

$$\frac{\partial \mathbf{B}}{\partial t} = -\nabla \times \mathbf{E} \quad (5)$$

The electric field is found using the fluid electron momentum equation, which is in this case called a generalized Ohm's law or GOL [*Priest*, 1982; *Siscoe*, 1983; *Cravens*, 1997]:

$$\mathbf{E} = -\mathbf{u} \times \mathbf{B} + \frac{1}{n_e e} \mathbf{J} \times \mathbf{B} - \frac{1}{n_e e} \nabla p_e + \eta \mathbf{J} + \text{small inertial terms} \quad (6)$$

where the Ohmic resistivity is given by

$$\eta = \frac{m_e \nu_e}{n_e e^2} \quad (7)$$

m_e is the electron mass, e is the magnitude of the electron charge, and ν_e is the sum of the electron-ion and electron-neutral collision frequencies. Expressions for the various electron and ion collision frequencies (with neutrals or ions) used in this paper can be found in *Keller et al.* [1992, 1994] or in *Schunk and Nagy* [2000].

[14] The first term on the right-hand side (RHS) of equation (6) is the motional electric field, the second term is the Hall field, the third term the polarization field, the fourth term the Ohmic resistivity term, and the last term accounts for inertial effects (usually neglected). Often, all but the motional and Ohmic terms are neglected and equations (5) and (6) together take the form of a convection-diffusion equation for the time evolution of the magnetic field:

$$\frac{\partial \mathbf{B}}{\partial t} = \nabla \times (\mathbf{u} \times \mathbf{B}) - \nabla \times (D_B \nabla \times \mathbf{B}) \quad (8)$$

where the magnetic diffusion coefficient, D_B , is given by:

$$D_B = \eta / \mu_0 = \frac{m_e \nu_e}{\mu_0 n_e e^2}. \quad (9)$$

The first term on the RHS accounts for transport of magnetic flux due to plasma flow, and the second term is a magnetic diffusion term. As explained in numerous textbooks, for the ideal MHD case (no resistivity), $D_B = 0$ and magnetic flux is said to be “frozen” into the plasma flow. *Keller et al.* [1994] determined for Voyager conditions that the electrical resistivity becomes large enough below about 1000 km in the ionosphere [*Keller et al.*, 1994] for the magnetic diffusion term to become important (i.e., Ohmic dissipation of electrical currents takes place).

[15] In this paper we estimate the relative importance of the magnetic “convection” and diffusion terms in equation (8) and we also estimate other terms in equation (7). The transport time constant for the magnetic field (or for the plasma in general) is given by $\tau \approx L/u$, and the magnetic diffusion time is of the order of $\tau_D \approx L^2/D_B$. The magnetic Reynold's number is the ratio of the diffusion time to the convection/transport time constant and is given by $R_m \approx Lu/D_B$. The appropriate length scale for magnetic diffusion in the lower ionosphere, where this is relevant, is almost certainly the vertical scale, L_{ver} , and this will later be used in these estimates. For large values of R_m the field is frozen into the flow. We will confirm that the $R_m \approx 1$ transition occurs somewhere between 800 and 1000 km for Titan.

[16] At Titan, the Hall and polarization terms can also be important in the ionosphere, and are, in fact, included in the global Hall MHD model of Titan of *Ma et al.* [2007]. We will also present estimates of these “nonstandard” MHD terms [cf. *Siscoe*, 1983] using:

$$\left(\frac{\delta \mathbf{B}}{\delta t}\right)_{\text{nonStd}} = -\frac{1}{n_e e} \nabla n_e \times \nabla (p_e + p_B). \quad (10)$$

The polarization part of equation (10) can be rewritten as:

$$\begin{aligned} \left(\frac{\delta \mathbf{B}}{\delta t}\right)_{\text{nonStd}} &= -\frac{k_B}{n_e e} \nabla n_e \times \nabla T_e \\ &\approx \frac{k_B T_e}{e} \frac{1}{L_{\text{hor}}} \frac{1}{L_{\text{ver}}} \end{aligned} \quad (11)$$

where L_{ver} is a vertical scale-length and L_{hor} a horizontal scale-length. As discussed by *Shinagawa et al.* [1993] with reference to the ionosphere of Venus, the polarization term is small if variations in the electron density and temperature are primarily vertical, but for regions (i.e., at dawn or dusk) with significant horizontal variations in n_e (and primarily vertical variations in T_e) then measurable magnetic fields can be produced. To summarize this discussion, equation (11) suggests that for maximum effect of the polarization term the gradients in electron density and temperature should be orthogonal.

3. Cassini Data for the Ionosphere

[17] Data from several Cassini flybys are used to make estimates of various quantities discussed in the last section. We have chosen T5 (nightside), T17 (dayside), and T18 (the terminator region). We also looked at data from another nightside flyby (T21) but the results were similar to the T5 results and we will not show them. Neutral densities measured by the Ion and Neutral Mass Spectrometer (INMS) for the major species (N_2 and CH_4) are used in finding the

collision frequencies needed in both the momentum and electrical resistivity terms. INMS neutral density measurements are described by *Magee et al.* [2009] and *Cui et al.* [2009a], and the densities we used (for day and night) are essentially the same as presented in these two papers.

[18] Electron densities and temperatures are also needed and we used values measured by the Radio and Plasma Wave Science (RPWS) Langmuir Probe as described by *Wahlund et al.* [2005] and *Ágren et al.* [2007]. The single-fluid MHD approach does not require knowing the detailed ion composition, but we assume that the average ion mass is ≈ 29 amu (C_2H_5^+ and HCNH^+ are particularly important species in Titan's chemically complex ionosphere) in line with Cassini INMS ion composition measurements [*Cravens et al.*, 2006]. The total ion densities measured by the INMS are in overall agreement with the RPWS electron densities except below 1000 km or so, where ion species heavier than 100 amu appear to be abundant (and were not measured by the INMS). Magnetic field information from the Cassini MAG experiment is used [e.g., *Backes et al.*, 2005; *Bertucci et al.*, 2008].

3.1. Nightside—T5

[19] Figure 1 is a schematic of the magnetospheric interaction with Titan for the T5 encounter and the Cassini trajectory (as seen in projection from above). Figure 2 shows electron densities and temperatures measured during the outbound portion of the T5 flyby by the Cassini RPWS Langmuir probe [cf. *Ágren et al.*, 2007]. The densities and temperatures measured for T5 inbound are very similar to outbound values. Furthermore, the RPWS electron densities agree well with the total ion density measured by the INMS below an altitude of about 1500 km [see *Ágren et al.*, 2007, and *Cravens et al.*, 2006].

[20] Figure 3 shows density profiles for N_2 and CH_4 measured by the INMS for T5 outbound.

[21] Figure 4 shows some magnetic field components measured by the Cassini MAG experiment for T5 (inbound and outbound) in TIIS coordinates (x is in the nominal corotation direction, y is toward Saturn, and z completes the right-handed coordinate system, i.e., northward). The magnetic field near CA is oriented with respect to the radial direction by about 45° ; that is, the field has a large radial component. This is a bit surprising given that the trajectory is in the ram part of the satellite for the interaction (see Figure 1) and that from models one would naively expect the magnetic field to be draped and to be almost horizontal [e.g., *Ma et al.*, 2006]. The observed presence of magnetic structure deep in the ionosphere evident in Figure 4 (also observed on other passes) suggests that the magnetic field extends into the lower atmosphere (below the spacecraft closest approach) and perhaps into the lower atmosphere and interior.

[22] Figures 2–4 show various quantities for T5 plotted versus altitude, but as mentioned earlier, the spacecraft spends about 600 s below an altitude of 1500 km (from inbound, through closest approach (CA) at 1027 km to outbound) and during this time it travels about 3000 km, mostly horizontal. Latitude, ram angle, and solar zenith angle all change along this track in addition to altitude.

[23] Thermal pressures ($p_{\text{th}} = p_e + p_i = n_e k_B (T_e + T_i)$) were calculated using the measured quantities shown in Figure 2

T5 Flyby Geometry

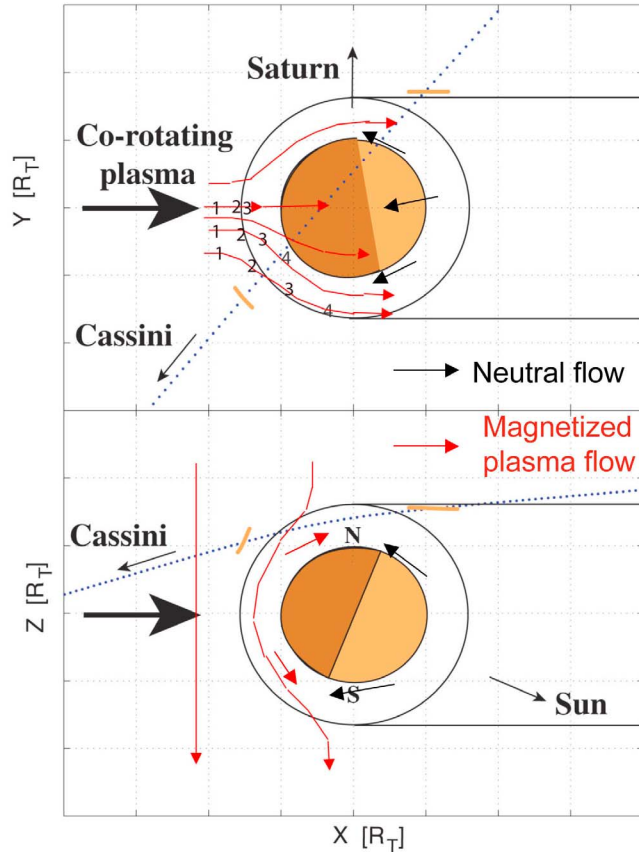


Figure 1a. Schematic of magnetospheric interaction with Titan during the T5 encounter as viewed from above the Saturnian equatorial plane and from the side. Cassini traveled through the polar nightside ionosphere. Some schematic plasma streamlines are shown in red and some possible day-to-night neutral wind directions are shown as black arrows. Adapted from *Ågren et al.* [2007].

plus an ion temperature of 200 K (this is ≈ 50 K in excess of the neutral temperature). Only one set of measured ion temperatures exists for Titan and, with large scatter, shows that below about 1500 km T_i is about equal to the neutral temperature of ≈ 150 K and that above this altitude T_i begins to increase [Crary *et al.*, 2009]. In any case, T_e significantly exceeds T_i in the ionosphere [Roboz and Nagy, 1994] and our approximation should be reasonable. Magnetic pressure ($B^2/2\mu_0$) was calculated with the data shown in Figure 4 (outbound). The T5 outbound pressures are shown in Figure 5. Thermal and magnetic pressures are comparable below about 1200 km and both slowly increase with altitude (or, more accurately increase along the spacecraft track outbound). The total pressure is not constant along this track so that a force imbalance exists that drives plasma downward along this track (and perhaps also in some unknown direction perpendicular to the track).

[24] T21 is a nightside pass for which the electron density is about half what it is for T5, but like T5 the thermal and magnetic pressures are comparable at low altitudes. Our dynamical deductions for this pass were quite similar to those for T5 and we will not show the results.

3.2. Dayside—T17

[25] The T17 Cassini flyby occurred entirely on the dayside and the peak electron density was high in comparison with T5 (i.e., $n_e \approx 3000 \text{ cm}^{-3}$ versus about 1000 cm^{-3}). T17 also took place in the downstream and wake region of the magnetospheric interaction. The electron temperature was not too different during T17 than during T5 (1000 K within 50% or so). The magnetic field strength below 1500 km was quite low on T17 (a couple of nT or less). Figure 6 shows pressures plotted versus altitude. Thermal pressure significantly exceeds magnetic pressure below 1500 km.

3.3. Terminator Region—T18

[26] Closest approach for the T18 flyby took place near the terminator (solar zenith angle $\approx 91^\circ$) and the outbound pass took place in a “twilight” dayside ionosphere. Figure 7 displays RPWS densities and temperatures and Figure 8 displays the magnetic field. Not surprisingly, densities are larger

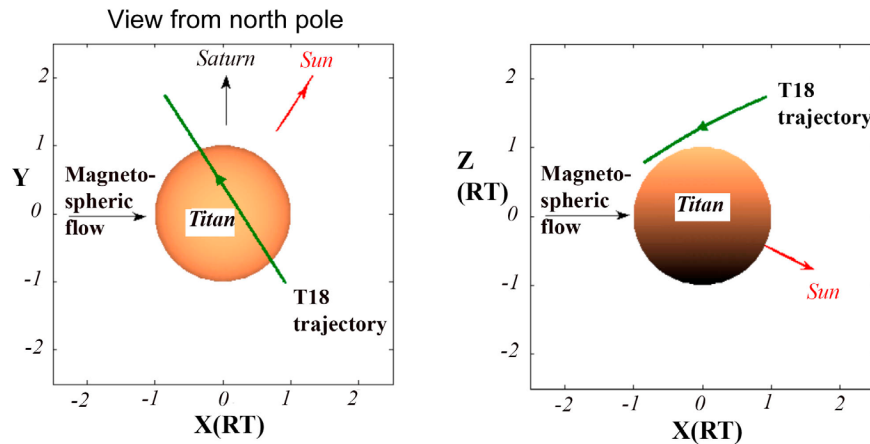


Figure 1b. Schematic of magnetospheric interaction with Titan during the T18 encounter.

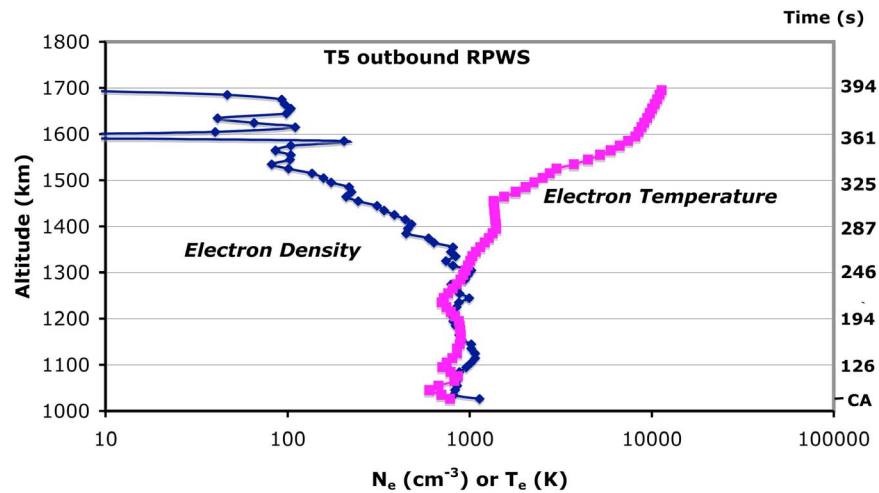


Figure 2. Electron density and temperature versus altitude measured by the Cassini RPWS Langmuir probe for T5 outbound. The time at Cassini along the outbound trajectory is shown on the right-hand side.

for T18 than for T5 but less than for T17 [Ågren *et al.*, 2009]. For T18, the magnetic field near CA is oriented almost horizontally (i.e., this is consistent with draping) with a field-strength of about 5 nT. Recall that the upstream magnetospheric conditions at Titan can vary significantly from flyby to flyby (compare reviews by Gombosi *et al.* [2009] and Mitchell *et al.* [2009]). Figure 9 shows calculated pressures. Thermal pressure dominates over magnetic pressure in the altitude range between 1000 km and 1500 km, but magnetic pressure is more important both at lower and higher altitudes. The total pressure is not constant along the track, although the variations are both positive and negative.

[27] For each flyby in this study we calculated the magnetic diffusion coefficient using the collision frequency formulae given by Keller *et al.* [1994] plus neutral and plasma densities (and temperatures). Figure 10 shows the calculated diffusion coefficient for the T18 outbound pass.

4. Empirical Estimates of Flow Speeds and Time Constants in the Ionosphere

[28] The dynamical equations presented in section 2 were combined with Cassini data in order to estimate ionospheric flow speeds. The velocity estimates require knowing the pressure gradients, but this is difficult to do with just measured data along the spacecraft track without knowing the 3-D structure of the ionosphere. That is, do the measured variations represent changes in pressure (or some other quantity) in the radial and vertical direction or in the horizontal direction, or a combination of both (plus perhaps intrinsic time variations)? We adopt two extreme assumptions, which might “bracket” the real situation: (1) that the variations are entirely vertical with a single scale-length L_{ver} (chosen to be ≈ 100 km as discussed later), or (2) that the variations are entirely horizontal with the scale-length L_{hor} (chosen to be ≈ 500 km as discussed later). Admittedly, these scales are somewhat arbitrary, but we will choose values that are plausible, and in some ways might represent minimum and maximum scales rather than strictly “vertical” or “horizontal” scales.

[29] Consider first some variations of measured electron density and temperature for T5 (Figure 2). The electron density decreases by a factor of two between 1400 and 1500 km—a vertical length scale of ≈ 100 km. On the other hand, the electron density is almost constant between about 1100 km and 1400 km (i.e., a vertical scale-length in excess of ≈ 300 km). Perhaps more relevant are the pressure variations shown in Figure 5. The total pressure has a significant variation over a vertical distance of $L_{\text{ver}} \approx 100$ km. Figure 5 also includes, on the righthand side, a scale showing the spacecraft time on the outbound leg of T5. Near closest approach the spacecraft is mostly moving horizontally at a speed of close to 6 km s^{-1} . A significant pressure variation is evident over a time period of ≈ 100 s which corresponds to a distance along the spacecraft track of $L_{\text{hor}} \approx 500\text{--}600$ km.

[30] Similar reasonable L_{ver} and L_{hor} estimates were made for the T17 and T18 passes. For example, the electron density for T17 (Figure 6) near 1200 km decreases by a factor of two to three over a 100 km altitude range. Similar variations can be seen in the T18 pressures (Figure 9). But again, if we assume that the variations are mainly horizontal then the appropriate scale-length is close to ≈ 500 km rather

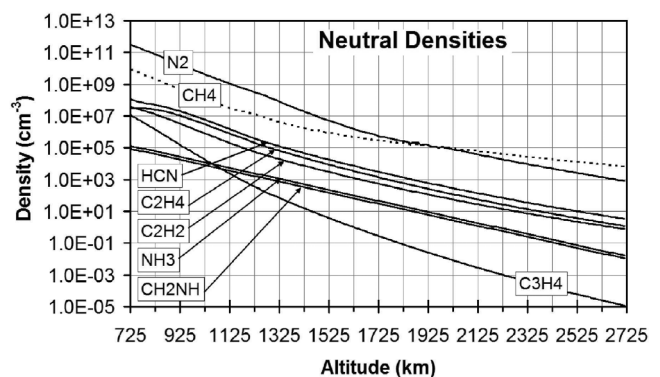


Figure 3. Densities of molecular nitrogen and methane versus altitude measured by the Cassini INMS for T5 outbound. Modified from Cravens *et al.* [2008b]; copyright 2008, with permission from Elsevier.

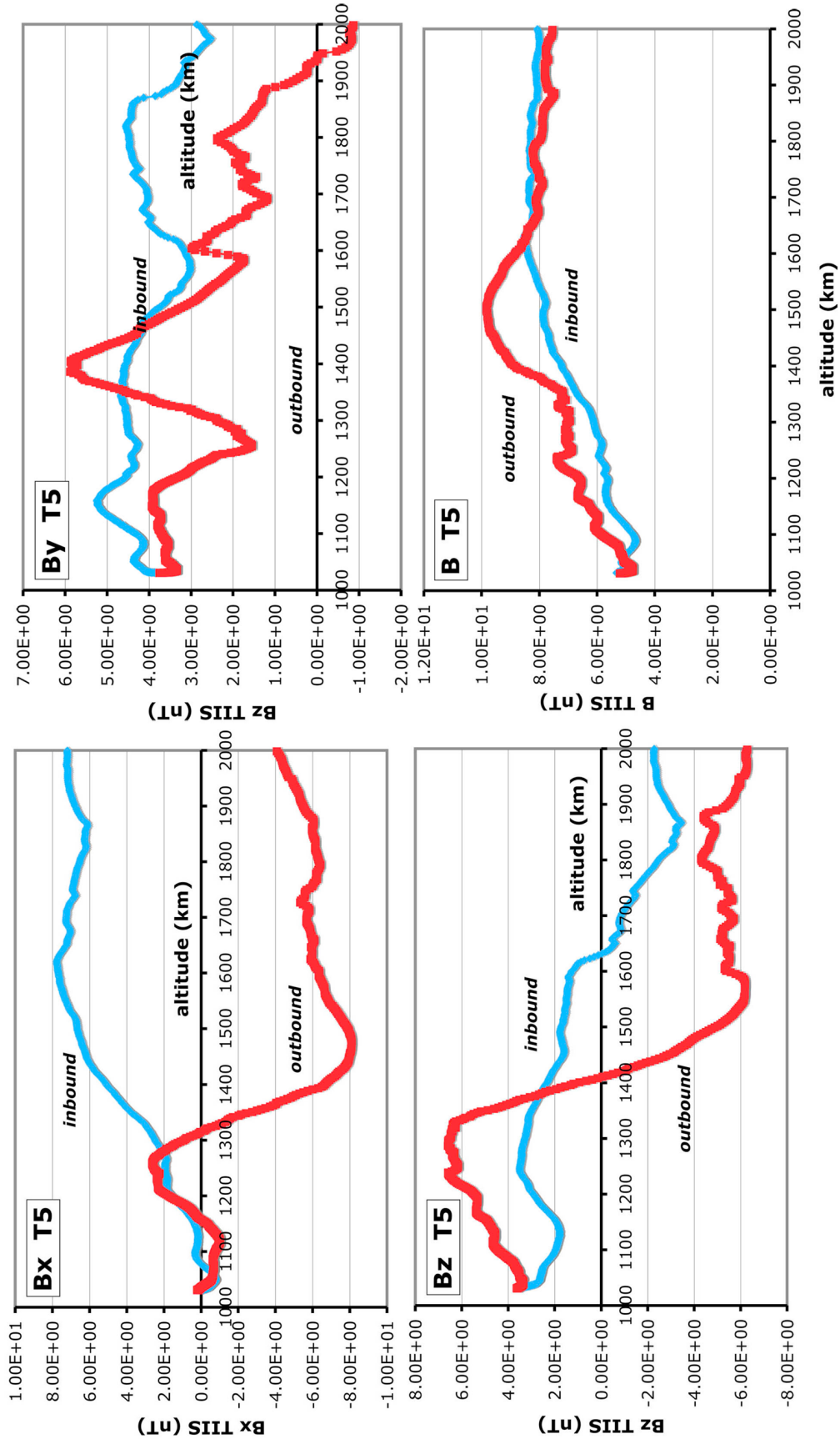


Figure 4. Magnetic field components in TIS coordinates and total magnetic field strength for T5 (inbound and outbound) measured by the Cassini MAG experiment.

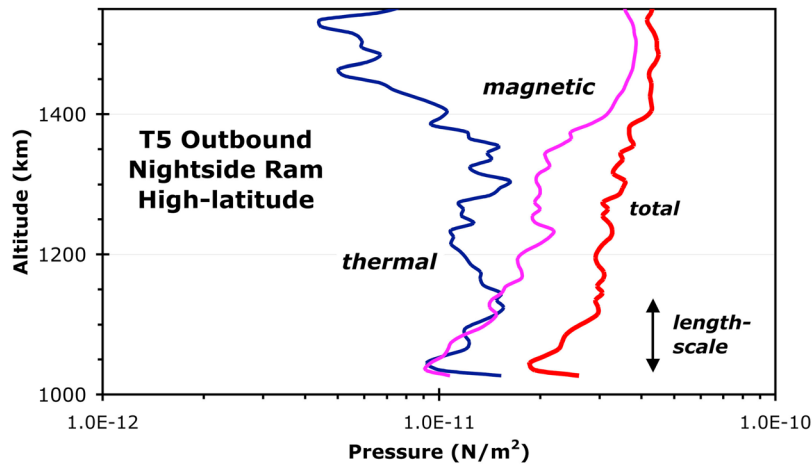


Figure 5. Thermal and magnetic pressures for T5 outbound and total pressure calculated using Cassini data. Total pressure is also shown. A length-scale bar is shown that corresponds both to 100 km and to a spacecraft time of about 120 s (see Figure 2).

than ≈ 100 km. The data figures in *Cravens et al.* [2008b] for T5 and in *Robertson et al.* [2009] for T17 and T18 provide both vertical and horizontal scales. Figure 7 in the current paper also shows a time scale from which a distance along the spacecraft track (roughly horizontal) of $L_{hor} \approx 500$ km can be seen to be reasonable.

[31] In addition to using estimated length scales, for T5 and T17 we also directly applied equation (3) to the vertical direction and evaluated the pressure gradients using $dp/dz \approx \Delta p/\Delta z$ with $\Delta z = 10$ km. The velocities produced by an unbalanced gravity term (only the ρg term on the righthand side of equation (3)) were also estimated. The overall ion flow velocity is a combination of \mathbf{u}' and the neutral wind velocity (\mathbf{u}_n), and the figures also show characteristic vertical ($w_n \approx 10$ m/s) and horizontal ($u_n \approx 100$ m/s) [cf. *Muller-Wodarg et al.*, 2000, 2003, 2008; J. M. Bell et al., Simulating the global mean structure of Titan’s upper atmosphere using the Titan global ionosphere-thermosphere model, submitted to *Planetary and Space Science*, 2009]

flow speeds, although these are probably more like upper limits, depending on latitude and local time.

[32] The results from these estimates will be shown in the following sections.

4.1. Estimates for T5 (Nightside)

[33] Figure 11 shows estimated vertical and horizontal flow speeds ($u' = |\mathbf{u} - \mathbf{u}_n|$) for T5. The smooth “gravity only” plasma speed profile and “horizontal” speed profile are similar. The “vertical” speeds are about five times greater than the horizontal speeds due to the smaller length-scales adopted for the former. The curve with the large excursions is the absolute magnitude of the vertical component of \mathbf{u}' found by estimating the derivative of pressure with respect to altitude. The velocity changes from positive to negative several times (not all shown), but it is overall negative (i.e., downward) and has values roughly bounded by the smoother vertical and horizontal speed curves. Small-scale excursions in the data being used are generating

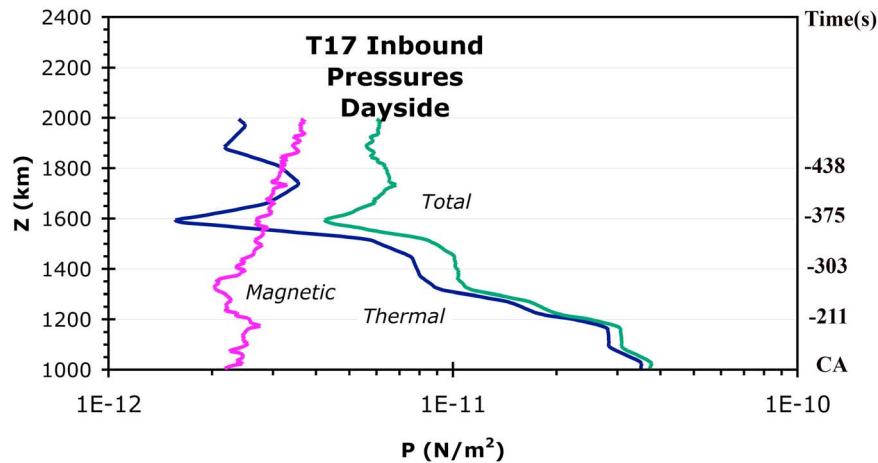


Figure 6. Thermal and magnetic pressures for T17 inbound and total pressure calculated using Cassini data. The time at Cassini along the inbound trajectory is shown on the right-hand side.

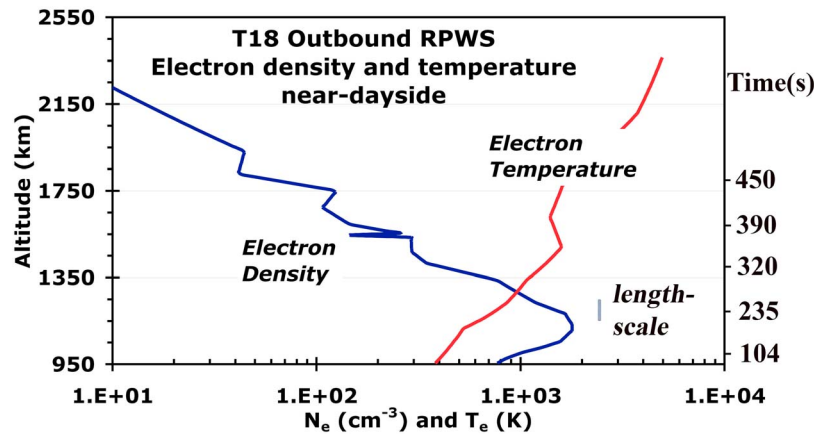


Figure 7. Electron density and temperature versus altitude measured by the Cassini RPWS Langmuir probe for T18 outbound. A scale for time from spacecraft closest approach on outbound is shown on the right-hand side. And a 100 km vertical length scale is shown just above the ionospheric peak.

small-scale structures in this velocity and should not be given much credence.

[34] The curve labeled “Ma et al.” is the total plasma flow speed versus altitude profile near the flanks from a numerical global MHD simulation for T5 (but without a neutral wind) [cf. *Ma et al.*, 2007]. A detailed comparison is not appropriate between the global MHD model and our estimates, but note that the global model speeds are approximately the same as our empirically estimated speeds.

[35] Flow speeds increase with altitude for all cases, which is due to the decrease of the ion-neutral collision frequency with altitude (i.e., in the denominator of equation (3)). The u' flow speed is about 1 m s^{-1} near 1000 km and increases to $\approx 100 \text{ m}^{-1} \text{ s}$ near 1300–1400 km. The flow speed begins to exceed the magnetosonic speed above 1500 km, indicating that the “diffusion approximation” that we used to derive equation (3) has become inappropriate. A dimensional analysis of the single-fluid momentum equation (equation (1)) shows that the ratio of the inertial terms (i.e., the left-hand side of the equation) to the pressure gradient terms on the righthand side is of the order of the magnetosonic Mach number squared [cf. *Siscoe*, 1983]. Thus, if this Mach number is small then it is a reasonable approximation to neglect the lefthand side, in which case equation (3) is a reasonable approximation. Note that equation (3) plus the continuity equation gives a diffusion-type equation [cf. *Cravens*, 1997].

[36] Thermospheric winds might also contribute to the ionospheric flow because of the u_n term in equation (3). That is, ion-neutral collisions tend to couple the plasma and neutrals, particularly at lower altitudes where this collision frequency is high. Thermospheric wind speeds and directions depend on many variables such as altitude, local time, and latitude. There are no clear-cut measurements of these winds at Titan and numerical thermospheric general circulation models differ in their predictions [*Muller-Wodarg et al.*, 2000, 2003; *Bell et al.*, submitted manuscript, 2009], but reasonable characteristic speeds are 100 m s^{-1} horizontally and 10 m s^{-1} vertically. These two speeds are indicated in Figure 11. The neutral flow speeds for T5 become comparable to u' values (that is, $|u_n - u_n|$) for altitudes below ≈ 1250 – 1350 km. The overall plasma veloc-

ity equals u' plus the neutral wind velocity, u_n , and the overall plasma flow velocity is evidently dominated by neutral winds at lower altitudes and by the plasma forcing (including the $\mathbf{J} \times \mathbf{B}$ term) at higher altitudes. Note that the neutral velocity and u' are not generally going to be in the same direction. In fact, during T5, for which CA is on the ramside (and on the nightside), the neutral and “plasma” flows should be roughly oppositely directed which could lead to interesting effects near an altitude of 1300 km (perhaps a stagnation layer?).

[37] Figure 12 shows the dynamical time constants (i.e., transport times associated with vertical or horizontal flow and magnetic diffusion times) calculated using our empirically estimated flow speeds. In finding these time constants, possible stagnation effects were neglected and the magnitudes of u' and u_n (or w_n) were simply added to find total speeds. Also shown is the magnetic diffusion time as will be discussed later. *Cravens et al.* [2008b] showed very similar transport time constants estimated in the same way but only including the u' speeds. *Cravens et al.* [2008b] also showed

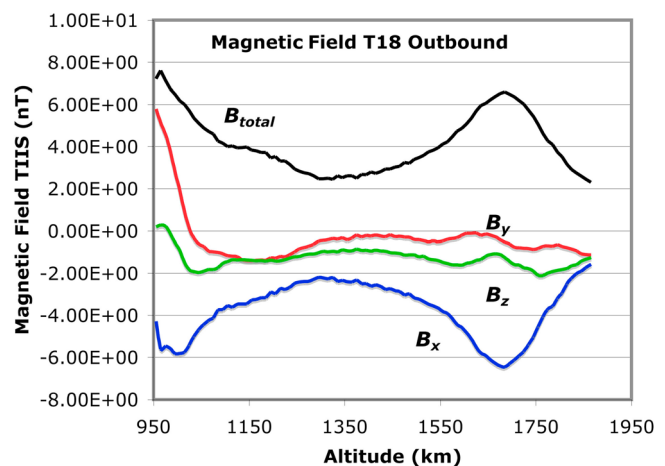


Figure 8. Magnetic field components in TIIS coordinates and total magnetic field strength for T18 outbound measured by the Cassini MAG experiment.

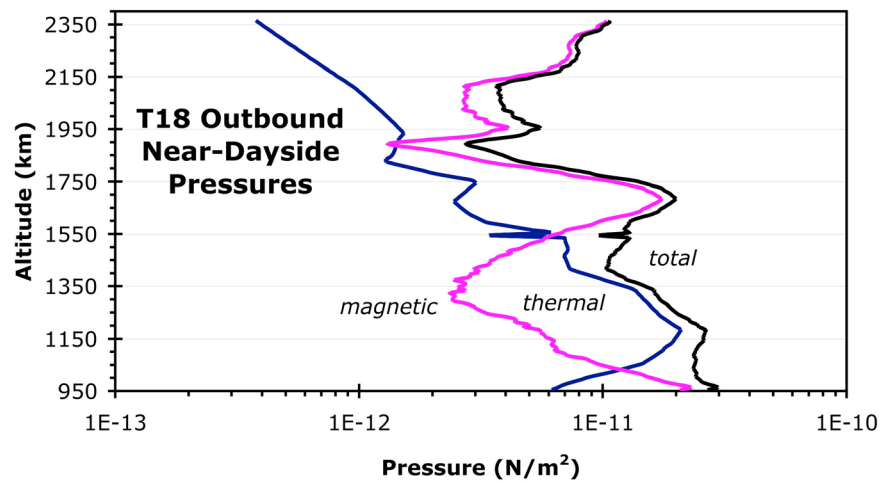


Figure 9. Thermal and magnetic pressures for T18 outbound and total pressure calculated using Cassini data.

chemical lifetimes for several species. Chemical lifetimes will be discussed again later in the paper.

4.2. Estimates for T17 Inbound (Dayside) and T18 Outbound (Dayside/Terminator)

[38] Figure 13 shows estimated vertical and horizontal flow speeds for the dayside/terminator ionosphere, and Figure 14 shows the associated time constants. Figures 15 and 16 show the dynamical information for the dayside (T17). Overall, flow speeds and dynamical/transport time constants estimated for the dayside are similar to those estimated for T5. Note, however, that vertical velocities relative to the neutral velocities (that is, \mathbf{u}') tend to be upward for the dayside and downward for the nightside (not shown). And just as on the nightside, neutral winds are potentially important for ion transport for altitudes below ≈ 1300 km. With typical neutral flow speeds taken into account, the magnetic diffusion time becomes comparable to, or less than, the transport time only for altitudes below about 1000 km.

5. Discussion of Ionospheric Dynamics

5.1. Chemical Versus Dynamical Control of Ionospheric Structure

[39] The density of an ion species, s , in a planetary ionosphere can be described with the continuity equation [cf. *Schunk and Nagy, 2000*]:

$$\frac{\partial n_s}{\partial t} + \nabla \cdot (n_s \mathbf{u}_s) = P_s - L_s \quad (12)$$

where P_s is the production rate of species s , including “primary” production from photoionization and/or electron impact ionization and production from chemical reactions. L_s is the loss rate of species s including ion-neutral reactions and electron-ion recombination reactions. The flow velocity of ion species s is denoted by \mathbf{u}_s , and this quantity can be determined from a momentum equation for this individual species (an equation similar to equation (1)) [see *Schunk and Nagy, 2000* or *Cravens, 1997*]. As discussed earlier, a single-

fluid description of the plasma is often useful. The major ion species will tend to have velocities close to the single fluid flow velocity ($\mathbf{u}_s \approx \mathbf{u}$). In any case, where \mathbf{u} (or \mathbf{u}_s) is small, such as at low altitudes, then a photochemical equilibrium approximation to the continuity equation becomes accurate and the resulting set of equations ($P_s = L_s$) can be solved to find ion densities (and hence, the total ion density or electron density, n_e). On the other hand, for flow velocities, \mathbf{u}_s (or \mathbf{u}) that are sufficiently high, or for small net production rates, the transport of ions and plasma must be taken into account.

[40] It has long been recognized that the approximate dividing line between chemical and dynamical control for the ionosphere for Titan is located at an altitude of ≈ 1400 km [e.g., *Keller et al., 1994*; *Cravens et al., 1998, 2008b*; *Robertson et al., 2009*; *Ma et al., 2004*; see review by *Cravens et al., 2009*]. Figure 17 shows chemical and dynamical/transport time constants for several ion species for the terminator region of Titan (T18). Transport appears to be important for long-lived ion species (e.g., HCNH^+ , CH_2NH_2^+) at altitudes as low as 1200 km, whereas for chemically short-lived species (e.g., N_2^+ , C_2H_5^+) the transition is located at higher altitudes near 1500 km, although the transition altitudes could be somewhat higher since the

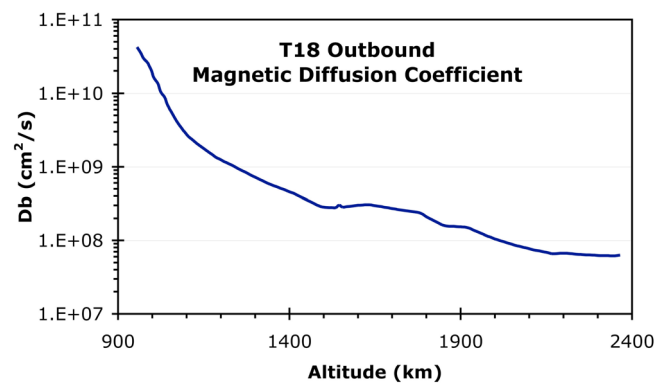


Figure 10. Magnetic diffusion coefficient versus altitude for T18 outbound.

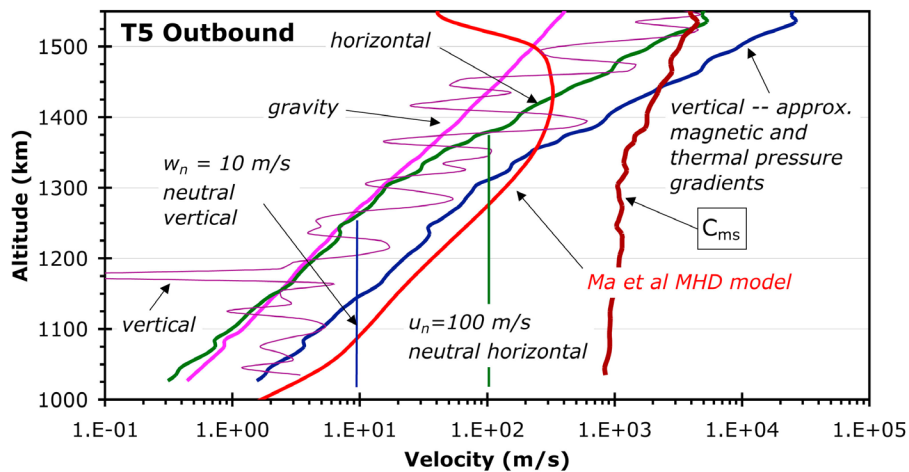


Figure 11. Estimated ionospheric flow speeds for T5 outbound. The curves marked vertical and horizontal are speeds (u') estimated using length scales of 100 km and 500 km, respectively. The absolute magnitude of the vertical ion velocity calculated using dp/dz is shown and is labeled “vertical.” A total plasma flow speed from a global MHD model for T5 [cf. *Ma et al.*, 2006, 2007] is shown. “Typical” vertical and horizontal neutral wind speeds are shown. The velocity estimated without pressure gradients but with just the gravity term is also shown. C_{ms} is the magnetosonic speed found using the empirical data.

length-scales are likely in some places to be greater than the 100 km length-scale adopted here.

5.2. Sources of Titan's Nightside Ionosphere

[41] *Robertson et al.* [2009] demonstrated, using a photochemical model that has 73 ion species and several hundred reactions, that only a solar radiation source of ionization was needed to explain measured dayside ionospheric densities during T17 and T18, out to solar zenith angles of about 100° . However, *Robertson et al.* did not completely explain the complex ionospheric chemical details [cf. *Carrasco et al.*, 2006; *Vuitton et al.*, 2007; *Krasnopolsky*, 2009].

[42] *Cravens et al.* [2008b] and *Ågren et al.* [2007] showed that on the nightside for T5 and T21, electron impact ionization by precipitating magnetospheric electrons was the key local ionospheric source. Note that magnetospheric electron fluxes were particularly high during T5 when Titan was within Saturn's magnetospheric plasma-sheet [*Rymer et al.*, 2009]. Using sets of ion density profiles measured by the INMS and averaged over several flybys to examine day-to-night density ratios, *Cui et al.* [2009b] deduced that day-to-night transport must also contribute to the densities of chemically long-lived ion species (e.g., CH_2NH_2^+) on the nightside. Short-lived species exhibit larger day-to-night density ratios than do long-lived ion species. *Cravens et al.* [2008b] were able to at least partially reproduce measured densities of both long-lived and short-lived ion species for T5 using both photochemical and time-dependent models without including day-to-night transport but including auroral energetic electron precipitation. That is, comparing the results of a nightside photochemical model [*Cravens et al.*, 2009] to those of a dayside model [i.e., *Robertson et al.*, 2009], we find smaller day-to-night ratios for long-lived species than for short-lived species. This can be expected just as a consequence of longer dissociative recombination lifetimes for such species on the

nightside (i.e., lower electron densities) than on the dayside (i.e., higher electron densities). Nonetheless, transport effects, as discussed by *Cui et al.* [2009b], should be taken into account when modeling Titan's nightside ionosphere. This is supported by an examination of the estimated time constants (Figure 17), which show that transport times for ion species such as CH_2NH_2^+ are comparable to chemical lifetimes at altitudes as low as 1200 km. Clearly, systematic model-data comparisons including both nightside in situ ionization sources [i.e., *Cravens et al.*, 2008a, 2008b; *Ågren et al.*, 2007] and transport effects [e.g., *Cui et al.*, 2009b] are called for.

[43] Ideally one could use a global dynamical model of the magnetospheric interaction with Titan but including a sophisticated chemical scheme and other aeronautical

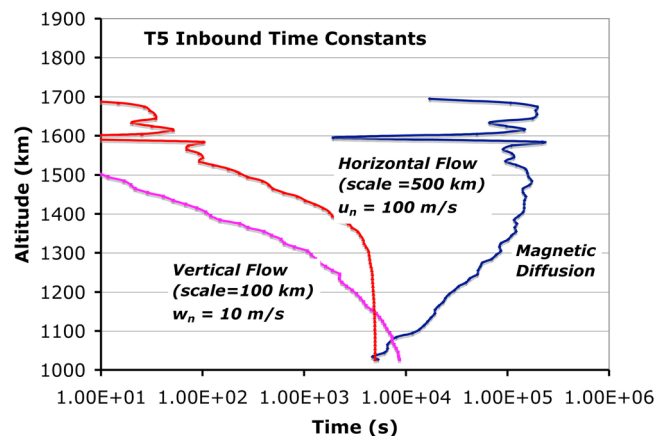


Figure 12. Estimated time constants for both vertical and horizontal transport for T5 outbound determined using Figure 11 speeds that included the neutral wind speeds. The length scales used in the estimated speeds are indicated. Magnetic diffusion time versus altitude is also shown.

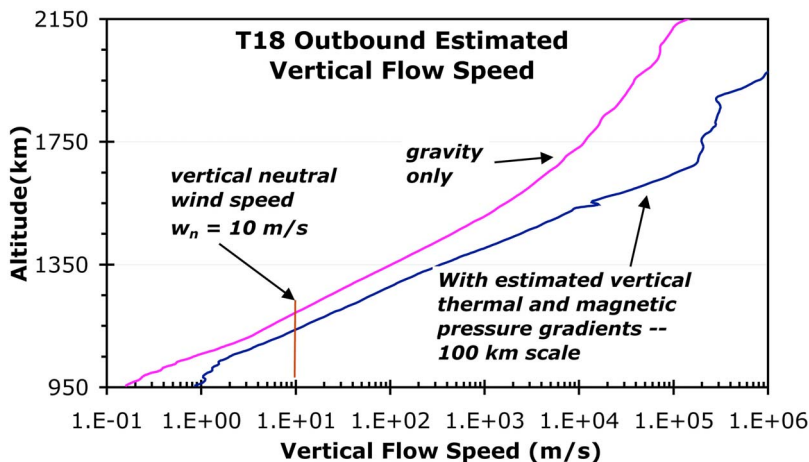


Figure 13. Estimated vertical ionospheric flow speeds for T18 outbound (near terminator dayside). Both \mathbf{u}' and a neutral vertical wind speed of 10 m s^{-1} are shown. The gravity only ion flow velocity is also shown.

processes. The 3-D MHD model of *Ma et al.* [2006, 2007] currently includes seven “generic” ion species as well as some chemistry, and dayside and nightside ion production. In an improved model the ionospheric dynamics would also include both the \mathbf{u}' plasma flow component (plasma and magnetic forcing) and the neutral component (\mathbf{u}_n), perhaps found using a dynamical model of the thermosphere [Muller-Wodarg et al., 2003; Bell et al., submitted manuscript, 2009]. The way magnetospheric and solar orientations combine could lead to interesting ionospheric dynamical effects. For example, when the magnetospheric flow (i.e., ram direction) more or less aligns with the solar direction, then both \mathbf{u}' and \mathbf{u}_n will align and ionospheric plasma will simply move from day to night in a Venus-like scenario [cf. Cravens et al., 1983]. But when they oppose, a shear/stagnation layer could result.

[44] Venus has some lessons for Titan. Two sources of the nightside ionosphere were proposed for Venus and vigorously debated: (1) in situ ionization due to precipitating solar wind electrons (actually magnetosheath electrons), and (2) transport of plasma from the dayside to the nightside, mainly in the form of O^+ ions. Fluxes of electrons (energies of 100 eV or less) were detected on the nightside by the plasma detector on the Veneras 9 and 10 spacecraft and were sufficiently high to produce ionospheric densities of a few thousand cm^{-3} [Gringauz et al., 1979]. Day-to-night O^+ flow speeds of a few km s^{-1} were measured in the topside Venus ionosphere by the retarding potential analyzer on the Pioneer Venus Orbiter [e.g., Knudsen et al., 1980]. The O^+ ions have large chemical lifetimes above 200 km so that plasma is able to survive the journey from the dayside (where solar radiation creates plasma) to the nightside. On the nightside these ions diffuse downward and react with CO_2 , thus producing O_2^+ ions (the major ion species measured at the peak, both on the day and the night). Two-dimensional modeling demonstrated that for low or moderate solar wind dynamic pressures, when the ionopause height is located above about 500 km, day-to-night transport could explain most of the nightside ionosphere, whereas when the solar wind dynamic pressure was high (and the ionopause located at lower altitudes), then the transport source did not

work [Cravens et al., 1983]. Perhaps both transport and in situ ionization effects are contributing to the formation of Titan’s nightside ionosphere [e.g., Cui et al., 2009b] just as at Venus.

5.3. Relative Roles of the Neutral and Plasma/Field Forces for Ionospheric Plasma Flow

[45] The external plasma flow ram and the solar directions do not always align at Titan, unlike the Venus scenario. The T5 flyby appears to be one such case (see Figure 1). For T5, the neutral flow is probably directed from low to high latitudes and/or from day to night, although the thermospheric neutral dynamics are not yet well understood [e.g., Muller-Wodarg et al., 2000, 2003, 2006, 2008]. The part of $\mathbf{u}' = \mathbf{u} - \mathbf{u}_n$ associated with thermal pressure gradient should mainly be in the day to night direction, but the part of \mathbf{u}' due to magnetic pressure gradients will mainly be directed away from the ram direction (i.e., from night to day). The $\mathbf{J} \times \mathbf{B}$

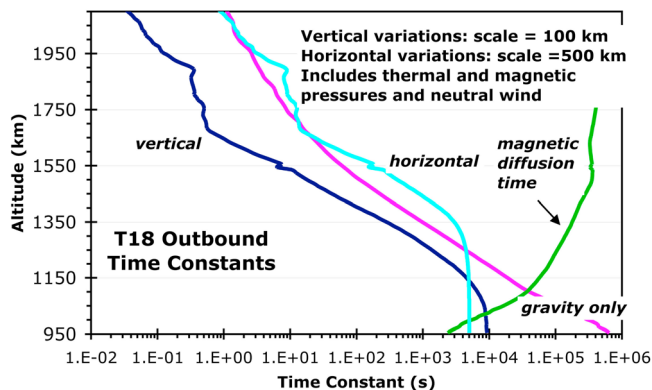


Figure 14. Estimated time constants for both vertical and horizontal transport for T18 outbound determined using estimated speeds that included the neutral wind speeds. The time constant for vertical speed that was determined only with gravity and ion-neutral friction is also shown. The length scales used in the estimated speeds are indicated. Magnetic diffusion time versus altitude is also shown.

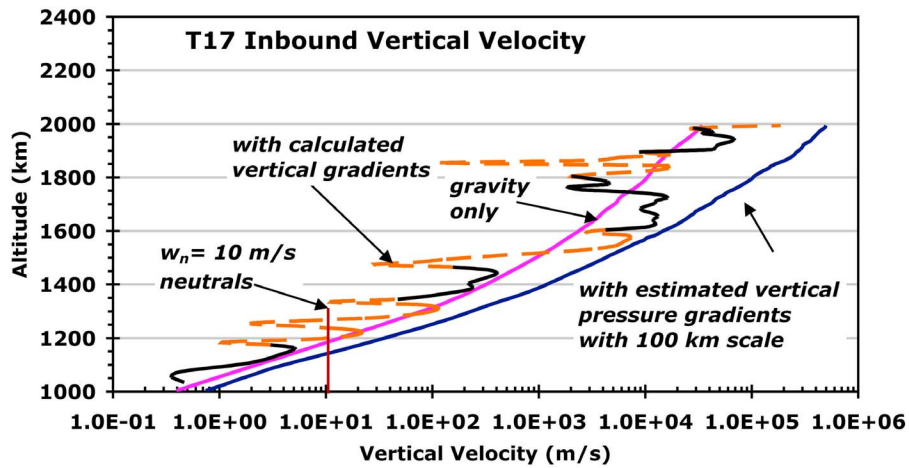


Figure 15. Estimated vertical ionospheric flow speeds for T17 inbound (middle of dayside). Both u' and a neutral vertical wind speed of 10 m s^{-1} are shown. The ion flow velocity due only to the gravitational force balanced by friction is also shown. The vertical flow velocity found using the calculated vertical pressure gradient (as opposed to a simple length scale) is shown—the solid lines are downward velocities and the dashed lines are upward velocities.

term (i.e., magnetic pressure) should dominate at higher altitudes. Considering the estimates in Figure 11, a stagnation region sometimes exists near an altitude of roughly 1300 km, where the magnitudes of u' and u_n are comparable. The effects of transport on ionospheric structure could be quite different below and above this transition altitude.

6. Discussion of the Ionospheric Magnetic Field

6.1. Role of Magnetic Diffusion in Titan's Ionosphere: Magnetic Reynold's Number

[46] The induced magnetic field appears to have an overall draped pattern with some pile-up on the ramside and the formation of a magnetic tail on the wakeside [e.g.,

Backes et al., 2005; Bertucci et al., 2008; Ma et al., 2006]. However, the details of the actual measured field are evidently complex and not fully described as just simple draping, particularly at lower altitudes.

[47] For example, consider the T32 Cassini flyby of Titan, when the satellite was located outside Saturn's magnetopause in the magnetosheath but had previously been inside the magnetosphere. The magnetic field measured in the ionosphere exhibited characteristics indicating that it had been induced in the ionosphere during an earlier time period when Titan was in the magnetosphere [Bertucci et al., 2008]. Note that Neubauer et al. [2006] introduced the concept of "fossil" magnetic fields in their discussions of Titan's magnetic field. These measurements of "fossil" magnetic fields in the ionosphere demonstrate that non-

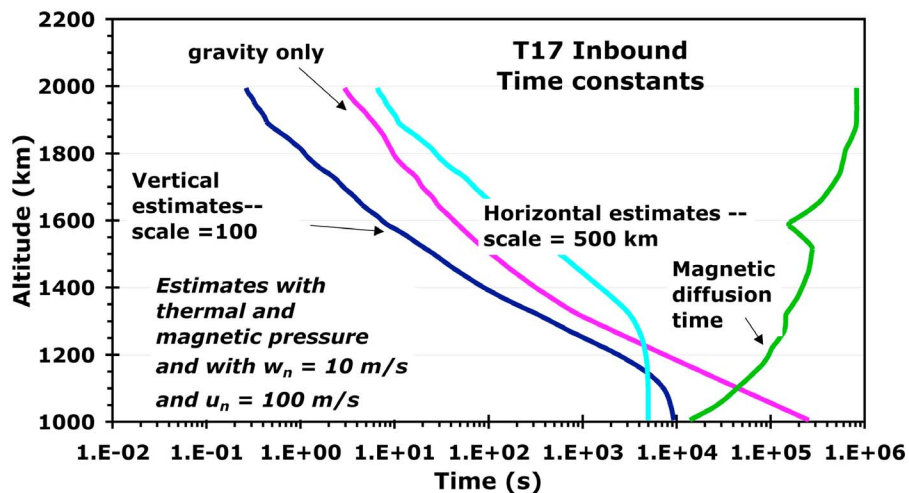


Figure 16. Estimated time constants for both vertical and horizontal transport for T17 outbound determined using estimated speeds that included the neutral wind speeds. The time constant for vertical speed that was determined only with gravity and ion-neutral friction is also shown. The length scales used in the estimated speeds are indicated. Magnetic diffusion time versus altitude is also shown.

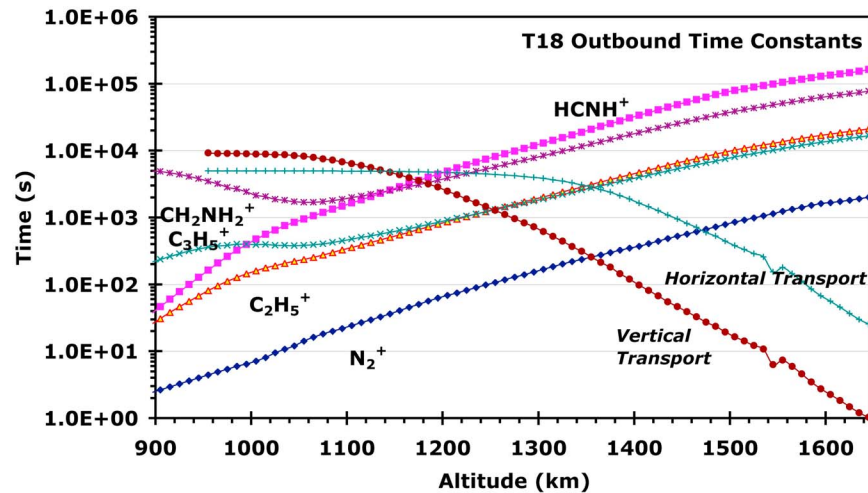


Figure 17. Estimated chemical lifetimes and transport time constants (horizontal and vertical) for the ionosphere of Titan on the dayside near the terminator for T18 conditions. The estimated vertical transport time constant from Figure 14 is included, as are chemical time constants for representative chemical species (short-lived, e.g., N_2^+ and $C_2H_5^+$, and long-lived, e.g., $CH_2NH_2^+$ and $HCNH^+$). Modified from Robertson *et al.* [2009]; copyright 2009, with permission from Elsevier.

stationarity of upstream plasma and field conditions can strongly affect the induced magnetic field patterns in the ionosphere (and thus also affect the dynamics as the current paper has discussed).

[48] The “convection” term in the magnetic induction equation (8) is dominant outside the ionosphere, and even in most of the ionosphere. Combined with the flow of plasma around Titan, this term results in a draping pattern [cf. Ledvina and Cravens, 1998; Ma *et al.*, 2006]. However, within the ionosphere itself other terms in equations (5) and (6) also need to be taken into account. These terms are the polarization electric field, the Hall, and the Ohmic resistivity terms.

[49] First, we use the empirical estimates of time scales presented earlier to estimate the magnitudes of the magnetic diffusion and convection terms for Titan’s ionosphere. The ratio of the magnetic convection time to the magnetic diffusion time is known as the magnetic Reynold’s number [cf. Siscoe, 1983; Cravens, 1997]—denoted R_m . Convection dominates where R_m greatly exceeds unity, and where R_m is of the order of unity or less, then magnetic diffusion dominates. At Venus, for example, one finds that $R_m \gg 1$ in the topside ionosphere but that $R_m \approx 1$, or less, for altitudes of about 150 km or lower. Data-model comparisons indeed demonstrated that magnetic diffusion (i.e., Ohmic dissipation) was an important process in the lower ionosphere of Venus [Cravens *et al.*, 1984; Shinagawa and Cravens, 1989; see the review by Luhmann and Cravens, 1991]. For high solar wind dynamic pressure conditions, magnetic flux is convected downward from the magnetic barrier (i.e., bottom of the magnetosheath) into the ionosphere (as well as antisunward from day to night). Magnetic fields are generated throughout the ionosphere by this convection process, but the fields are dissipated below about 150 km (where $R_m \approx 1$).

[50] Keller *et al.* [1994] adopted a multispecies, 1-D MHD approach to studying the magnetic field in Titan’s ramside ionosphere, using the methods of Shinagawa and

Cravens [1988, 1989]. Keller *et al.* demonstrated, at least for Voyager 1 conditions, that magnetic diffusion becomes important only below an altitude of ≈ 1000 km (where $R_m \approx 1$). Keller *et al.* also noted that for conditions in which the ionospheric densities were quite low (i.e., such as on the nightside) then the magnetic field could extend throughout the ionosphere and not become zero even at the lowest altitudes. For a 1-D scenario (which is obviously not entirely accurate) with a purely horizontal magnetic field (also not really accurate even on the ramside), strong magnetic diffusion control of the field ($R_m \ll 1$) implies that (see equation (10)) $D_B dB/dz \approx 0$, which means that either $B = 0$ and/or $dB/dz \approx 0$ in the lower ionosphere where D_B is large. In other words, even if magnetic diffusion dominates, the magnetic field does not necessarily go to zero at lower altitudes below the main ionospheric layer. However, diffusion-dominated magnetic field profiles should not exhibit large gradients.

[51] We now re-examine the role of magnetic diffusion in the light of Cassini data using the empirically based transport time constants presented earlier. Figures 12, 14, and 16 show the empirically estimated transport time constants for the three Cassini flybys considered in this paper. We estimate the transition altitude where $R_m \approx 1$ (i.e., the altitude where the magnetic diffusion time is equal to the convection or transport time). Including the neutral flow speed (assumed to be roughly 100 m s^{-1}) as part of the estimated plasma flow speed, then the transition altitude is located near 1000 km for both T5 and T18 and is located somewhere below 1000 km for T17. But if we adopt a neutral wind velocity of zero, then the $R_m \approx 1$ transition altitude is at higher altitudes near 1100 km. The measured magnetic field profiles appear to exhibit sizeable vertical (and/or horizontal) gradients near closest approach, which suggests that magnetic diffusion is probably not yet the dominant process even near Cassini’s closest approach altitudes. This in turn suggests that the neutral wind makes an important contribution to the plasma/field transport near 1000 km, at least

for the three Cassini flybys considered in this paper. However, such a change of field direction (i.e., a current layer) could also be the sign of a fossil field directional discontinuity [Neubauer *et al.*, 2006; Bertucci *et al.*, 2009].

6.2. Role of the Hall Term in the Magnetic Induction Equation

[52] It is apparent from a comparison of standard and Hall global MHD models of the magnetospheric interaction with Titan that Hall effects are important in the ionosphere, although qualitatively the overall magnetic field draping pattern is not altered by these effects [Ma *et al.*, 2007]. Do empirical estimates of the Hall term in the magnetic induction equation (i.e., the magnetic pressure part of equation (10)) agree with these numerical results? We construct a “Hall” magnetic Reynold’s number, R_{mH} , by dividing the dimensional estimate of the transport time by the time constant for the Hall term in equation (10):

$$R_{mH} \approx n_e e u \mu_0 L / B \approx M_A \left[\frac{L}{r_{LiA}} \right] \quad (13)$$

where u is the plasma flow speed and L is the relevant length-scale for magnetic field variations (e.g., $L \approx 100$ – 500 km). M_A is the Alfvénic Mach number and r_{LiA} is an ion gyroradius calculated with the Alfvén speed. Hall effects are not important where $R_{mH} \gg 1$, but such effects need to be included for $R_{mH} \approx 1$ (or less).

[53] We estimated R_{mH} for Titan’s ionosphere below about 1300 km. Taking the ion flow speed to be roughly the neutral speed ($u \approx u_n \approx 100$ m s⁻¹), the electron density to be $n_e \approx 2000$ cm⁻³, a field strength of $B \approx 5$ nT, and a length scale in the range $L \approx 100$ – 500 km, we find that $R_{mH} \approx 0.7$ – 3.5 , indicating that Hall effects are indeed somewhat important below 1300 km, but not necessarily dominant. At Venus, a similar estimate gives $R_{mH} \approx 10$ in the ionosphere, indicating that the Hall term is less important for Venus than it is for Titan. The Hall MHD numerical simulations of Ma *et al.* [2007] also demonstrated the importance of the Hall term in the Titan interaction scenario.

6.3. Role of the Polarization Electric Field Term in the Magnetic Induction Equation

[54] The time rate of change of the magnetic field due to the polarization electric field term in the induction equation is given by the part of equation (10) containing the electron pressure, p_e . We estimated this contribution to the magnetic field evolution by using equation (11). The polarization term only makes a contribution to the induced magnetic field if the electron density gradient and electron temperature gradient are not entirely parallel. Our knowledge of the global variations of n_e and T_e is still incomplete [cf. Ågren *et al.*, 2009] but the largest variations in both these two quantities are in the radial and vertical directions. However, near the terminator the electron density also has a significant horizontal gradient [Ågren *et al.*, 2009], whereas the horizontal gradient in the electron temperature is not so dramatic. Adopting a vertical scale length of $L_{ver} \approx 100$ km for T_e variations and a scale length of $L_{hor} \approx 500$ km for horizontal n_e variations (for the ionosphere between 1000 km and 1500 km), equation (11) gives the following estimated value: $(\delta B / \delta t)_{polar} \approx 10^{-3}$ nT s⁻¹. Using an overall transport

time for the magnetic field of 10^4 s (see Figures 12, 14, 16), then the field generated by the polarization term could be as large as 10 nT, which is a typical measured magnetic field strength in Titan’s ionosphere. The direction of the magnetic field from the polarization effect near the dawn or dusk terminators should be parallel to the terminator (i.e., orthogonal to the sun-direction) according to equation (11), as also suggested for Venus by Shinagawa *et al.* [1993]. The polarization field contribution to the magnetic field might also be locally important near small-scale density structures found on the nightside and associated with spatially variable electron precipitation [Ågren *et al.*, 2007; Cravens *et al.*, 2008a].

6.4. Role of the Neutral Wind in the Control of the Ionospheric Magnetic Field

[55] We noted in section 5.3 that the plasma/field contribution (\mathbf{u}') to the ionospheric plasma flow velocity could act quite differently than the neutral wind (\mathbf{u}_n) contribution [Muller-Wodarg *et al.*, 2003, 2006, 2008]. In particular, we suggested that in some cases (e.g., perhaps for T5) the neutral wind and plasma and field parts of the plasma flow velocity could be oppositely directed and that this could create a stagnation and shear region near 1300 km. Not only is the distribution of plasma in the ionosphere affected by transport as discussed earlier, the structure of the magnetic field is determined by transport, thus indicating that below about 1300 km, thermospheric neutral winds are certainly important in determining the magnetic field structure. And in some situations, \mathbf{u}' and \mathbf{u}_n will oppose each other, thus producing what would otherwise be unexpected magnetic structure near the transition altitude. Perhaps the electric current layer (i.e., field change) evident near 1300 km in the measured magnetic field profiles for T5 (Figure 4) can be attributed to this effect.

7. Summary

[56] Empirical estimates of thermal and magnetic pressures, ion flow velocities, and time constants using T5, T17, and T18 Cassini data were provided and were used to make the following key points:

[57] 1. Thermal and magnetic pressure gradient forces opposed by ion-neutral “friction” force determine the flow velocity of ionospheric plasma relative to the neutral gas. This relative speed is quite small in the lower ionosphere (few m/s or less near 1000 km) but increases rapidly with altitude as the neutral density decreases.

[58] 2. Below about 1300 km, the neutral wind contribution to the overall plasma flow velocity should be dominant in most cases and needs to be included in any analysis or numerical model of Titan’s plasma environment.

[59] 3. At lower altitudes (below about 1300–1500 km, depending on location and on the ion species), ion-neutral chemical and dissociative recombination reactions control the ionospheric density structure, whereas at higher altitudes plasma transport becomes more important.

[60] 4. The nightside ionosphere is probably maintained both by in situ “auroral” ionization and by transport of plasma from the dayside.

[61] 5. The magnetic field structure in the ionosphere is determined by transport processes for altitudes above about

1000 km and by magnetic diffusion at lower altitudes. Below an altitude of roughly 1300 km, the neutral wind makes an important contribution to the transport of magnetic flux in the ionosphere.

[62] 6. The Hall effect [cf. Schunk and Nagy, 2000] makes a moderately important contribution to the structure of the induced magnetic field control in Titan's ionosphere (and has been included in some global MHD models) [Ma et al., 2007].

[63] 7. The polarization electric field term in the magnetic induction equation can be locally important, such as near the terminator, where it might produce a magnetic field aligned with the terminator. Correctly including this term in the magnetic induction equation requires knowledge of horizontal and vertical variations of the electron temperature and density.

[64] 8. When the ram direction of the external magnetospheric flow is very different from the Sun's direction, then the neutral wind direction and the magnetic forcing direction could be quite different in the ionosphere and lead to possible flow shear and/or stagnation layers (probably near 1300 km altitude), and these should affect the magnetic structure.

[65] 9. The external plasma interaction with Titan's ionosphere has several features in common with the solar wind interaction with Venus, but appears to be overall more complicated. For example, at both objects pressure gradients can drive ionospheric plasma flow, but whereas the flow direction at Venus is very much from day to night, at Titan the flow direction is not so obvious due to differences in the flow ram direction and the Sun's direction.

[66] **Acknowledgments.** This work has been supported at the University of Kansas by NASA grants NM0710023 via Cassini subcontract from the Southwest Research Institute and NASA grants NNX07AF47G and NNX10AB86G (Planetary Atmospheres). The authors thank the reviewers for very helpful comments.

[67] Robert Lysak thanks Fritz M. Neubauer and another reviewer for their assistance in evaluating this paper.

References

- Ågren, K., et al. (2007), On magnetospheric electron impact ionization and dynamics in Titan's ram-side and polar ionosphere, a Cassini case study, *Ann. Geophys.*, **25**, 2359.
- Ågren, K., J.-E. Wahlund, P. Garnier, R. Modolo, J. Cui, M. Galand, and I. Müller-Wodarg (2009), On the ionospheric structure of Titan, *Planet. Space Sci.*, **57**, 1821, doi:10.1016/j.pss.2009.04.012.
- Backes, H., F. M. Neubauer, M. K. Dougherty, H. Achilleos, N. Andre, C. S. Arridge, C. Bertucci, G. H. Jones, and K. K. Khurana (2005), Titan's magnetic field signature during the first Cassini encounter, *Science*, **308**, 992.
- Bertucci, C., et al. (2008), The magnetic memory of Titan's ionized atmosphere, *Science*, **321**, 1475.
- Bertucci, C., B. Sinclair, N. Achilleos, P. Hunt, M. K. Dougherty, and C. S. Arridge (2009), The variability of Titan's magnetic environment, *Planet. Space Sci.*, **57**, 1813, doi:10.1016/j.pss.2009.02.009.
- Brecht, S. H., J. G. Luhmann, and D. J. Larson (2000), Simulation of the Saturnian magnetosphere interaction with Titan, *J. Geophys. Res.*, **105**, 13,119.
- Carrasco, N., O. Dutuit, R. Thissen, M. Banaszekiewicz, and P. Pernot (2006), Uncertainty analysis of bimolecular reactions in Titan ionosphere chemistry model, *Planet. Space Sci.*, **55**, 141, doi:10.1016/j.pss.2006.06.004.
- Coates, A. J., F. J. Crary, D. T. Young, K. Szego, C. S. Arridge, Z. Bebesi, and E. C. Sittler Jr. (2007), Ionospheric electrons in Titan's tail: Plasma structure during the Cassini T9 encounter, *Geophys. Res. Lett.*, **34**, L24S05, doi:10.1029/2007GL030919.
- Crory, F. J., B. A. Magee, K. E. Mandt, J. H. Waite, J. Westlake, and D. T. Young (2009), Heavy ions, temperatures and winds in Titan's ionosphere: Combined Cassini CAPS and INMS observations, *Planet. Space Sci.*, **57**, 1847, doi:10.1016/j.pss.2009.09.006.
- Cravens, T. E. (1997), *Physics of Solar System Plasmas*, Cambridge Univ. Press, Cambridge, U. K.
- Cravens, T. E., S. L. Crawford, A. F. Nagy, and T. I. Gombosi (1983), A two-dimensional model of the ionosphere of Venus, *J. Geophys. Res.*, **88**, 5595.
- Cravens, T. E., H. Shinagawa, and A. F. Nagy (1984), The evolution of large-scale magnetic fields in the ionosphere of Venus, *Geophys. Res. Lett.*, **11**, 267.
- Cravens, T. E., C. N. Keller, and B. Ray (1997), Photochemical sources of non-thermal neutrals for the exosphere of Titan, *Planet. Space Sci.*, **45**, 889.
- Cravens, T. E., C. J. Lindgren, and S. A. Ledvina (1998), A two-dimensional multifluid MHD model of Titan's plasma environment, *Planet. Space Sci.*, **46**, 1193.
- Cravens, T. E., et al. (2006), The composition of Titan's ionosphere, *Geophys. Res. Lett.*, **33**, L07105, doi:10.1029/2005GL025575.
- Cravens, T. E., et al. (2008a), Energetic ion precipitation at Titan, *Geophys. Res. Lett.*, **35**, L03103, doi:10.1029/2007GL032451.
- Cravens, T. E., et al. (2008b), Model-data comparisons for Titan's night-side ionosphere, *Icarus*, **199**, 174, doi:10.1016/j.icarus.2008.09.005.
- Cravens, T. E., R. V. Yelle, J.-E. Wahlund, D. E. Shemansky, and A. F. Nagy (2009), Composition and structure of the ionosphere and thermosphere, in *Titan From Cassini-Huygens*, edited by R. H. Brown, J.-P. Lebreton, and J. H. Waite, chap. 11, p. 259, Springer, New York.
- Cui, J., et al. (2009a), Analysis of Titan's neutral upper atmosphere from Cassini Ion Neutral Mass Spectrometer measurements, *Icarus*, **200**, 581, doi:10.1016/j.icarus.2008.12.005.
- Cui, J., M. Galand, R. V. Yelle, V. Vuitton, J.-E. Wahlund, P. P. Lavvas, I. C. F. Müller-Wodarg, T. E. Cravens, W. T. Kasprzak, and J. H. Waite Jr. (2009b), Diurnal variations of Titan's ionosphere, *J. Geophys. Res.*, **114**, A06310, doi:10.1029/2009JA014228.
- Gombosi, T. I., T. P. Armstrong, C. S. Arridge, K. K. Khurana, S. M. Krimigis, N. Krupp, A. M. Peerson, and M. F. Thomson (2009), Saturn's magnetospheric configuration, in *Saturn From Cassini-Huygens*, edited by M. K. Dougherty, L. W. Esposito, and S. M. Krimigis, chap. 12, p. 203, Springer, New York.
- Gringauz, K. I., M. I. Verigin, T. K. Breus, and T. Gombosi (1979), The interaction of electrons in the optical umbra of Venus with the planetary atmosphere: The origin of the nighttime ionosphere, *J. Geophys. Res.*, **84**, 2123.
- Hartle, R. E., et al. (2006), Initial interpretation of Titan plasma interaction as observed by the Cassini Plasma Spectrometer: Comparisons with Voyager 1, *Planet. Space Sci.*, **54**, 1211.
- Ip, W.-H. (1990), Titan's upper ionosphere, *Astrophys. J.*, **362**(10), 354.
- Kabin, K., T. I. Gombosi, D. L. DeZeeuw, K. G. Powell, and P. L. Israelevich (1999), Interaction of the Saturnian magnetosphere with Titan, *J. Geophys. Res.*, **104**, 2451.
- Keller, C. N., and T. E. Cravens (1994), One dimensional multispecies hydrodynamic models of the wakeside ionosphere of Titan, *J. Geophys. Res.*, **99**, 6527.
- Keller, C. N., T. E. Cravens, and L. Gan (1992), A model of the ionosphere of Titan, *J. Geophys. Res.*, **97**, 12,117.
- Keller, C. N., T. E. Cravens, and L. Gan (1994), One dimensional multispecies magnetohydrodynamic models of the ramside ionosphere of Titan, *J. Geophys. Res.*, **99**, 6511.
- Knudsen, W. C., K. Spenner, K. L. Miller, and V. Novak (1980), Transport of ionospheric O⁺ ions across the Venus terminator and implications, *J. Geophys. Res.*, **85**, 7803.
- Krasnopolsky, V. A. (2009), A photochemical model of Titan's atmosphere and ionosphere, *Icarus*, **201**, 226.
- Ledvina, S. A., and T. E. Cravens (1998), A three-dimensional MHD model of plasma flow around Titan, *Planet. Space Sci.*, **46**, 1175.
- Ledvina, S. A., Y.-J. Ma, and E. Kallio (2008), Modeling and simulating flowing plasmas and related phenomena, in *Comparative Aeronomy*, edited by A. F. Nagy et al., p. 143, Springer, New York.
- Luhmann, J. G., and T. E. Cravens (1991), Magnetic fields in the ionosphere of Venus, *Space Sci. Rev.*, **55**, 201.
- Ma, Y.-J. (2008), Plasma flow and related phenomena in planetary aeronomy, in *Comparative Aeronomy*, edited by A. F. Nagy et al., p. 311, Springer, New York.
- Ma, Y.-J., A. F. Nagy, T. E. Cravens, I. V. Sokolov, J. Clark, and K. C. Hansen (2004), 3-D global MHD model prediction for the first close flyby of Titan by Cassini, *Geophys. Res. Lett.*, **31**, L22803, doi:10.1029/2004GL021215.
- Ma, Y.-J., A. F. Nagy, T. E. Cravens, I. U. Sokolov, K. C. Hansen, J.-E. Wahlund, F. J. Crary, A. J. Coates, and M. K. Dougherty (2006), Comparisons between MHD model calculations and observations of

- Cassini flybys of Titan, *J. Geophys. Res.*, *111*, A05207, doi:10.1029/2005JA011481.
- Ma, Y.-J., et al. (2007), 3D global multi-species Hall-MHD simulation of the Cassini T9 flyby, *Geophys. Res. Lett.*, *34*, L24S10, doi:10.1029/2007GL031627.
- Magee, B., J. H. Waite, K. E. Mandt, J. Bell, J. Westlake, D. A. Gell, and V. De la Haye (2009), INMS derived composition of Titan's upper atmosphere: Analysis methods and model comparison, *Planet. Space Sci.*, *57*, 1895, doi:10.1016/j.pss.2009.06.016.
- Mitchell, D. G., J. F. Carbary, S. H. Cowley, T. W. Hill, and P. Zarka (2009), The dynamics of Saturn's magnetosphere, in *Saturn From Cassini-Huygens*, edited by M. K. Dougherty, L. W. Esposito, and S. M. Krimigis, chap. 10, p. 257, Springer, New York.
- Modolo, R., and G. M. Chanteur (2008), A global hybrid model for Titan's interaction with the Kronian plasma: Application to the Cassini Ta flyby, *J. Geophys. Res.*, *113*, A01317, doi:10.1029/2007JA012453.
- Müller-Wodarg, I. C. F., R. V. Yelle, M. Mendillo, L. A. Young, and A. D. Aylward (2000), The thermosphere of Titan simulated by a global three-dimensional time-dependent model, *J. Geophys. Res.*, *105*, 20,833.
- Müller-Wodarg, I. C. F., R. V. Yelle, M. J. Mendillo, and A. D. Aylward (2003), On the global distribution of neutral gases in Titan's upper atmosphere and its effect on the thermal structure, *J. Geophys. Res.*, *108*(A12), 1453, doi:10.1029/2003JA010054.
- Müller-Wodarg, I. C. F., R. V. Yelle, J. Cui, and J. H. Waite (2008), Horizontal structures and dynamics of Titan's thermosphere, *J. Geophys. Res.*, *113*, E10005, doi:10.1029/2007JE003033.
- Neubauer, F. M., D. A. Gurnett, J. D. Scudder, and R. E. Hartle (1984), Titan's magnetospheric interaction, in *Saturn*, edited by T. Gehrels and M. S. Matthews, p. 760, Univ. of Ariz. Press, Tucson.
- Neubauer, F. M., et al. (2006), Titan's near magnetotail from magnetic field and electron plasma observations and modeling: Cassini flybys TA, TB, and T3, *J. Geophys. Res.*, *111*, A10220, doi:10.1029/2006JA011676.
- Priest, E. R. (1982), *Solar Magnetohydrodynamics*, D. Reidel, Dordrecht, Netherlands.
- Robertson, I. P., et al. (2009), Structure of Titan's ionosphere: Model comparisons with Cassini data, *Planet. Space Sci.*, *57*, 1843, doi:10.1016/j.pss.2009.07.011.
- Roboz, A., and A. F. Nagy (1994), The energetics of Titan's ionosphere, *J. Geophys. Res.*, *99*, 2087.
- Rymer, A. M., H. T. Smith, A. Wellbrock, A. J. Coates, and D. T. Young (2009), Discrete classification and electron energy spectra of Titan's varied magnetospheric environment, *Geophys. Res. Lett.*, *36*, L15109, doi:10.1029/2009GL039427.
- Schunk, R. W., and A. F. Nagy (2000), Simplified transport equations, in *Ionospheres: Physics, Plasma Physics, and Chemistry*, *Cambridge Atmos. Space Sci. Ser.*, edited by A. J. Dressler, J. T. Houghton, and M. J. Rycroft, p. 104, Cambridge Univ. Press, Cambridge, U. K.
- Shinagawa, H., and T. E. Cravens (1988), A one-dimensional multi-species magnetohydrodynamical model of the dayside ionosphere of Venus, *J. Geophys. Res.*, *93*, 11,263.
- Shinagawa, H., and T. E. Cravens (1989), A one-dimensional multi-species magnetohydrodynamical model of the dayside ionosphere of Mars, *J. Geophys. Res.*, *94*, 6506.
- Shinagawa, H., T. E. Cravens, and A. F. Nagy (1987), A one-dimensional time-dependent model of the magnetized ionosphere of Venus, *J. Geophys. Res.*, *92*, 7317.
- Shinagawa, H., T. E. Cravens, and D. Wu (1993), The generation of magnetic fields by the polarization electric field in the ionosphere of Venus, *J. Geophys. Res.*, *98*, 263.
- Sillanpaa, I., E. Kallio, P. Janhunen, W. Schmidt, Mursula, J. Vilpola, and P. Tanskanen (2006), Hybrid simulation study of ion escape at Titan for different orbital positions, *Adv. Space Res.*, *38*, 799.
- Simon, S., A. Boesswetter, T. Bagdonat, U. Motschmann, and J. Schuele (2007), Three-dimensional multispecies hybrid simulation of Titan's highly variable plasma environment, *Ann. Geophys.*, *25*, 117.
- Siscoe, G. L. (1983), Solar system magnetohydrodynamics, in *Solar-Terrestrial Physics: Principles and Theoretical Foundation*, edited by R. L. Carovillano and J. M. Forbes, p. 11, D. Reidel, Dordrecht, Netherlands.
- Vuittou, V., R. V. Yelle, and M. J. McEwan (2007), Ion chemistry and N-containing molecules in Titan's upper atmosphere, *Icarus*, *191*, 722.
- Wahlund, J.-E., et al. (2005), Cassini measurements of cold plasma in the ionosphere of Titan, *Science*, *308*, 986.
- K. Ågren and J.-E. Wahlund, Swedish Institute of Space Physics, Box 537, SE-751 21 Uppsala, Sweden.
- J. Bell and J. H. Waite, Southwest Research Institute, PO Drawer 28510, 6220 Culebra Rd., San Antonio, TX 78284, USA.
- C. Bertucci, Instituto de Astronomía y Física del Espacio, Ciudad Universitaria, Casilla de Correo 67, Suc. 28, Buenos Aires C1428ZAA, Argentina.
- T. E. Cravens, M. Richard, and I. P. Robertson, Department of Physics and Astronomy, University of Kansas, Lawrence, KS 66045, USA. (cravens@ku.edu)
- J. Cui, M. Dougherty, and I. Müller-Wodarg, Space and Atmospheric Physics Group, Blackett Laboratory, Imperial College London, London, SW7 2AZ, UK.
- S. Ledvina, J. G. Luhmann, and D. Ulusen, Space Sciences Laboratory, University of California, 7 Gauss Way, Berkeley, CA 94720, USA.
- Y.-J. Ma, Institute of Geophysics and Planetary Physics, University of California, 3845 Slichter Hall, Charles E. Young Dr. E., Los Angeles, CA 90025, USA.